

EXPERIMENTAL STUDY OF TURBULENT MACROINSTABILITIES IN AN AGITATED SYSTEM WITH AXIAL HIGH-SPEED IMPELLER AND WITH RADIAL BAFFLES

Oldrich BRUHA^{a1}, Ivan FORT^b, Pavel SMOLKA^{a2} and Milan JAHODA^c

^a Department of Physics, Czech Technical University, 166 07 Prague 6, Czech Republic;
e-mail: ¹ bruha@fsid.cvut.cz, ² smolka@fsid.cvut.cz

^b Department of Chemical and Food Process Equipment Design, Czech Technical University,
166 07 Prague 6, Czech Republic

^c Department of Chemical Engineering, Prague Institute of Chemical Technology, 166 28 Prague 6,
Czech Republic; e-mail: jahodam@vscht.cz

Received October 19, 1995

Accepted January 22, 1996

The frequency of turbulent macroinstability occurrence was measured in liquids agitated in a cylindrical baffled vessel. As it has been proved by preceding experimental results of the authors, the stochastic quantity with frequency of occurrence of 10^{-1} to 10^0 s^{-1} is concerned. By suitable choosing the viscosity of liquids and frequency of impeller revolutions, the region of Reynolds mixing numbers was covered from the pure laminar up to fully developed turbulent regime. In addition to the equipment making it possible to record automatically the macroinstability occurrence, also the visualization method and videorecording were employed. It enabled us to describe in more detail the form of entire flow field in the agitated system and its behaviour in connection with the macroinstability occurrence. It follows from the experiments made that under turbulent regime of flow of agitated liquids the frequency of turbulent macroinstability occurrence is the same as the frequency of the primary circulation of agitated liquid.

Key words: Macroinstability; Axial impeller; Mixing in transient region.

This work takes up papers^{1,2} which describe the phenomenon and basic properties of macroinstabilities in agitated systems. Attention has begun to be paid to this phenomenon in past several years at laboratories concerning with mixing processes³⁻⁸. The complex effect of macroinstabilities on the course of mixing process has not been, however, hitherto evaluated and the experiment concerning with the dynamic effects of macroinstabilities on mechanical parts of agitating system has hitherto been described in no paper. The main aim of this work was to investigate the dependence of frequency of macroinstability occurrence on the Reynolds mixing number in as wide as possible region of Re_M . In addition to it, the connection was examined in this work between the macroinstability occurrence and the changes of flow pattern in the region of the flow leaving the impeller. It is expected that results of these experiments will contribute to the elucidation of the origin of macroinstabilities itself.

EXPERIMENTAL

The experiments described in this work and in work² were carried out in the same experimental equipment, and for the investigation of macroinstability occurrence was used the same methodology. The extent of Reynolds mixing numbers at which the phenomenon was observed in the experiments described here, is, however, much wider and comprises both the transient region and the region of developed turbulence. The agitating device is schematically drawn in Fig. 1. It is a glass cylindrical flat-bottom vessel of diameter $D = 0.3$ m filled with the examined Newtonian liquid up to the level height $H = D$. The vessel was equipped at its wall with four radial baffles of the width $b = 0.1D = 0.03$ m. The impeller was a standard one, namely the pitched blade impeller with six inclined plane blades with the inclination angle of 45° . The impeller diameter $d = 0.3D = 0.1$ m and the frequency of revolutions $N = 3.33 \text{ s}^{-1}$ to 8.33 s^{-1} were chosen. The direction of rotation was chosen to pump the liquid always towards the vessel bottom. The liquid temperature was kept at the required value by means of an electric direct-heating element immersed into liquid and controlled by a thermostatic switch.

To make the flow field visible for direct observing and for video recording in the plane going through the vessel axis symmetrically between two adjacent baffles, the examined plane was illuminated with a light source emitting beam of light in the form of vertical band of width 5 mm (light knife). In this way, the particles-tracers (fine semolina or air bubbles) in the examined plane were sufficiently illuminated. It was possible to observe their motion visually, or if need be, to record with video camera and to analyze the record obtained later exploiting the possibility of repeating, decelerating or stopping the picture.

For an automatic and observer-independent record of macroinstability occurrence, an apparatus called tornadometer was used. This apparatus as well as the method of the record evaluation are described in more details in paper². In principle, the record depicts the time course of the force acting on a small target placed into the flow field in the region of instability occurrence. The suitable position for locating the target for each agitating regime was determined on the basis of criteria given in work². The axial off-bottom target coordinate was within $1.2H_2$ to $1.4H_2$. The radial coordinate was for all the agitating regimes practically the same and was approximately equal to the impeller radius. The effect of the off-bottom impeller clearance on the frequency of macroinstability occurrence may be generally expressed in terms of a so-called off-bottom clearance factor, as it is written in paper². Therefore, in experiments we confined in this work to only one impeller off-bottom clearance equal

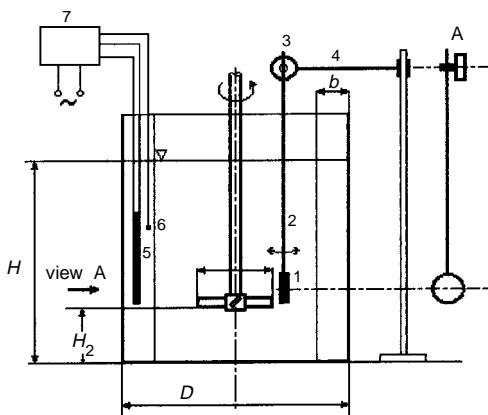


FIG. 1

Scheme of experimental arrangement. Parts of tornadometer: 1 Target, 2 swinging arm, 3 electric resistance sensor, 4 fixed arm. Parts of heating system: 5 Electroheating element, 6 temperature sensor, 7 heating control box

$H_2 = 0.35D$. This distance was considered in work² to be an impeller reference position for it is most often used in practice.

The liquids used in experiments were chosen so as to cover, by a suitable choice of concentration and temperature of aqueous glycerol solutions, a wide region of Reynolds mixing numbers $Re_M \in (210; 67\ 000)$, where

$$Re_M = \frac{Nd^2\rho}{\mu} \quad (1)$$

The temperature of agitated charge t was kept with an accuracy of 0.5 °C, the entire range of charge temperatures was 23 to 50 °C. The survey of liquids used and of their physical properties is given in Table I. For the density and viscosity of water, the tabular values were employed, for glycerol and its aqueous solutions, these values were measured*.

As a substance-tracer for making flows visible, fine food semolina of grain diameter to 0.1 mm was used for liquids with lower viscosity (water, 27 and 46% aqueous glycerol solutions). The semolina grains after sprinkling into liquid, mildly swelled but then they were stable in shape all the time of experiment. For liquids with higher viscosity (70% aqueous glycerol solution, concentrated glycerol) which are less transparent, and semolina seems to be little contrast, air bubbles of diameter up to 1 mm were used, generated by an aerating device used in aquaria. The air bubbles kept up in these more viscous liquids sufficiently long and were thoroughly visible.

Reproducibility and Accuracy of Measurement

For measuring the frequency of macroinstability occurrence and for processing the results of measurement, the method described in detail in paper² was used. Such as in the experiments described in paper², also in this work, the systematic errors of measurement were negligible compared to the random errors conditioned by the statistical character of the quantity measured. By using the method described in paper², the standard relative deviation was determined for each series; its value was in no case higher than 15%.

All the measurements were at least once repeated after one to four weeks, and the differences between the results of the initial and repeated measurements reached the maximum value of 20%.

RESULTS AND DISCUSSION

The results of performed measurements confirmed the conclusions of paper² concerning the dependence of mean frequency of macroinstability occurrence, \bar{f} , on the Reynolds mixing number and substantially extended the region of Re_M in which this dependence was investigated. In a diagram in Fig. 2, which depicts the dependence of mean dimensionless frequency of macroinstability occurrence

$$\bar{f}^* = \bar{f}/N \quad (2)$$

* Densities of aqueous glycerol solutions presented in Table I of paper² were estimated approximately on the basis of tabular values of pure substances and therefore they differ from the measured values.

on the Reynolds mixing number Re_M , the points are plotted corresponding to the results of measurements carried out by means of tornadometer. It is apparent from the figure that the above-mentioned property can be divided into three regions:

TABLE I
Physical properties of liquids used

Liquid/Solution	Temperature t , °C	Viscosity μ , mPa s	Density ρ , kg m ⁻³
Water	23	0.94	998
27% Saccharose in water	23	2.2	1 068
46% Saccharose in water	23	9.5	1 117
70% Glycerol in water	50	16	1 166
	45	20	1 169
	40	26	1 171
	35	33	1 173
	32	39	1 175
	30	44	1 176
	28	49	1 177
	27	51	1 178
	25	58	1 178
	23	59	1 179
Glycerol	50	100	1 240
	45	139	1 243
	40	195	1 246

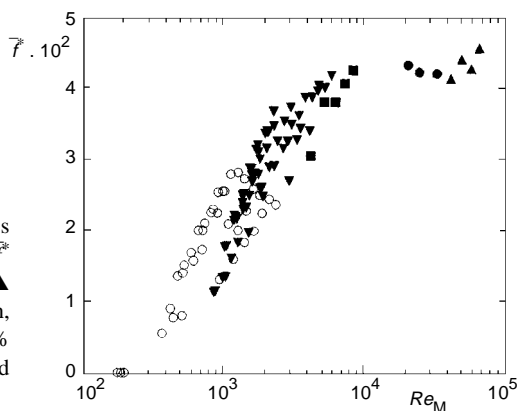


FIG. 2
Dependence of mean value of dimensionless frequency of macroinstability occurrence \bar{f} on Reynolds mixing number Re_M for: ▲ water, ● 27% aqueous saccharose solution, ■ 46% aqueous saccharose solution, ▼ 70% aqueous glycerol solution, ○ concentrated glycerol

– For $Re_M \leq 200$ when the flow in agitated liquid is laminar, macroinstabilities do not occur. The overall pattern of flow in this region is characterized by the main (primary) flow loop brought about by impeller (see the left-hand side A of Fig. 1 in paper²).

– For $Re_M \in (200; 5\,000)$, which corresponds to the transient region of flow, a unique trend of increasing values of quantity \bar{f} with increasing Re_M is apparent despite a certain dispersion of single points. It would be possible to approximate this dependence, e.g., by a logarithmic dependence. The physical interpretation of the character of course of this dependence, however, has not hitherto been known, and its analytical expression therefore was neither sought.

– In the region of developed turbulence for $Re_M > 9\,000$, the dimensionless frequency of macroinstability occurrence does not nearly change (at least up to the maximum examined value of Re_M), and its value may be considered in this region to be constant and lying in the interval of 0.043 to 0.048. It is in agreement with the results given in paper² where the value of slope of the straight line approximating the dependence of mean frequency of macroinstability occurrence on the impeller revolutions lies in the range of 0.041 to 0.05.

Making the flow field visible by inserting particles-tracers made it possible to record, document and additionally analyze its course during all the regimes investigated. In Fig. 3, the primary loop I induced by impeller is illustrated schematically. For investigating changes of its geometry in dependence on the intensity of agitating process, two characteristic points were chosen denoted here by A and B: Point A lies on the periph-

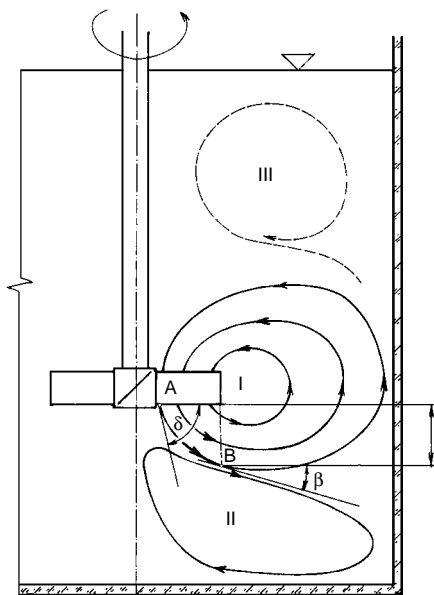


FIG. 3
To the definition of position of points A and B and angles δ and β . Primary flow loop I, stable secondary flow loop under impeller II, originating unstable secondary loop III

ery of the primary flow loop at the place of its outlet of impeller. From the visual observation follows that the radial coordinate of point A is practically identical with the impeller hub radius. Point B is a point lying on the periphery of primary loop as well under the impeller in the distance from vessel axis equal to the impeller radius. The axial distance of point B from the lower impeller edge depends on the form of primary loop, and its value which is determined separately for each agitating regime was within the range of 15 to 40 mm. Angles δ and β are angles between the horizontal plane and vectors of flow velocities (tangents to the edge streamline of primary flow loop) at points A and B). The edge of flow loop, passing at the discharge flow from impeller at point A, is the boundary of primary flow pumped directly by impeller and the secondary flow II. This originated in the lower vessel region, under impeller and does not flow through the body of rotating impeller. Points A and B were chosen in this way because their position which is bound to the impeller geometry and to the form of flow field, can be uniquely defined for all regimes of flow. The determination of angles δ and β was very difficult especially in the regime of turbulent agitating. When reading the angles on the screen, a correction for optical distortion caused by the cylindrical shape of the vessel was applied.

The values of angle δ in dependence on Re_M are illustrated in Fig. 4. Their course corresponds to the hitherto knowledge of the character of flow outflowing from the impeller, see, e.g., refs^{9,10}. It is apparent from the figure that angle δ increases with increasing Re_M above its minimum value, which is about 26° at $Re_M = 200$, and in the examined region of Reynolds numbers reaches the maximum values between 60 and 70° . It means that the pitched blade impeller behaves for small Re_M (about up to 1 000) rather as a radial impeller (δ is lower than 45°) and only for Re_M greater than 1000 approaches to an axial impeller (δ is greater than 45°). No connection between the changes of angle δ and macroinstabilities, however, was found.

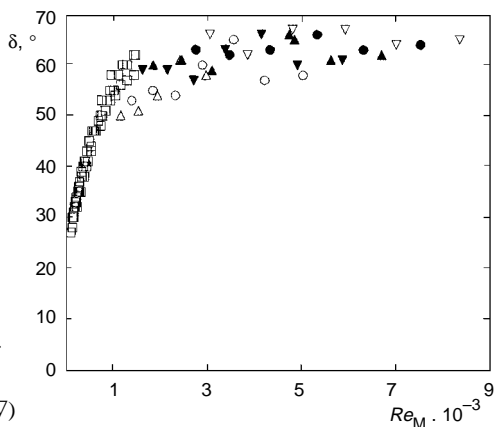


FIG. 4

Dependence of angle δ on Re_M for frequencies of impeller revolution $N = 4.2$ to 8.3 s^{-1} for concentrated glycerol and for 70% aqueous glycerol solution. Frequencies of impeller revolution N : 4.2 s^{-1} (Δ), 5 s^{-1} (\circ), 5.8 s^{-1} (∇), 6.7 s^{-1} (\blacktriangle), 7.5 s^{-1} (\bullet), 8.3 s^{-1} (∇)

For the study of macroinstability occurrence, the course of values of angle β is more interesting whose magnitude exhibits a connection with the overall shape of primary loop. This angle has unique values only for low Re_M (approximately to 1 000). From a certain value of Re_M , it is possible to determine for angle β only limiting values β_{\min} and β_{\max} within whose range its value varies with time. The determination of angle β was doubtlessly subject to a great error. Reading the angles from a TV monitor was carried out independently by three observers. Their data differed as much as 30% but showed the same trend of the dependence. In treating the measurements, the average value of this three observations was used. Figure 5 shows the results for measurements with concentrated glycerol, Fig. 6 the same dependence also for 70% aqueous glycerol solution and comprises in addition values from the preceding figure. The beginning of instability of primary loop signalled by a considerable dispersion of values of angle β , lies, as it is apparent from Figs 5 and 6, approximately at $Re_M = 800$. The existence of macroinstabilities was found out already at $Re_M = 200$ but despite it is possible to seek a certain connection between these two phenomena whose more detailed experimental study could elucidate the reasons of macroinstability formation. We did not manage to quantify precisely the frequency of "jumps" of angle β from the maximum value to the minimum value and vice versa with the used technique but only to estimate on the basis of visual observation within the range of 10^{-1} to 10^0 s^{-1} , therefore of the same order as the frequency of macroinstability occurrence in the system examined.

In the preceding papers^{1,2}, the macroinstabilities were described as a phenomenon accompanying the transition of flow regime of charge from single-loop to double-loop. The analysis of video records obtained during the above-mentioned experiments, however, shows that it is more suitable to speak on macroinstabilities as a manifestation of decay of the primary loop from which, at a certain instant of development, a part of it is released in the form of unstable secondary turbulent field having its own identity and

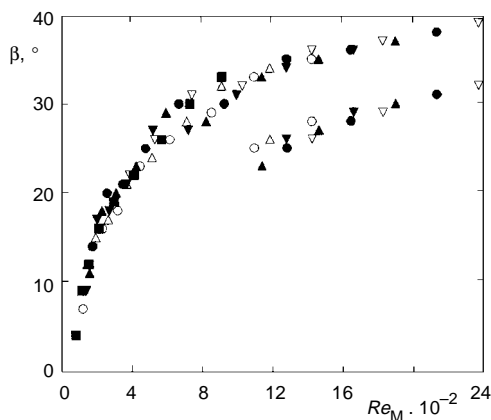


FIG. 5
Dependence of angle β on Re_M for concentrated glycerol. Frequency of impeller revolution N : 3.3 s^{-1} (■), 4.2 s^{-1} (△), 5 s^{-1} (○), 5.8 s^{-1} (▼), 6.7 s^{-1} (▲), 7.5 s^{-1} (●), 8.3 s^{-1} (▽)

moving towards the level (Fig. 3). The beginning of separation of the unstable secondary turbulent field from the primary loop and its further development is documented by photographs of the visualized flow field (Figs 7a, 7b). A more detailed study of properties of this unstable secondary turbulent field will form a subject of further research.

Primary loop of agitated liquid is, on the average, characterized by means of the mean time of primary circulation¹¹

$$t_c = \frac{V}{\dot{V}}, \quad (3)$$

where V is the volume of agitated liquid. Pumping capacity of impeller \dot{V} is, in a dimensionless form, expressed as the impeller flow rate number¹²

$$K_p = \frac{\dot{V}}{Nd^3}. \quad (4)$$

Quantity K_p does not depend, under turbulent regime of flow, on the Reynolds mixing number. Combination of Eqs (3) and (4) gives the dimensionless mean time of primary circulation

$$Nt_c = \frac{V}{K_p d^3} \quad (5)$$

and, finally, for the so-called "squared" mixing vessel ($H = D$) we have for the dimensionless mean frequency of primary circulation

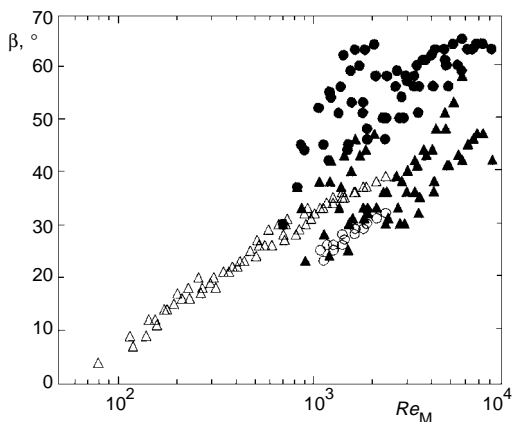


FIG. 6
Dependence of angles β_{\min} and β_{\max} on Re_M
for 70% aqueous glycerol solution (▲, ●)
and for concentrated glycerol (○, Δ)

$$F_c \equiv \frac{1}{Nt_c} = \frac{4}{\pi} K_p \left(\frac{d}{D} \right)^3. \quad (6)$$

From the results of experiments made with a flow follower in the same agitated system described in Experimental it follows that the impeller flow rate number depends on the impeller off-bottom clearance¹³

$$K_p = 0.7865(H_2/D)^{-0.19}, \quad d/D = 1/3, \quad Re_M > 5.0 \cdot 10^3. \quad (7)$$

Then, the combination of Eqs (6) and (7) gives, for the geometry of the agitated system investigated, the relation

$$F_c = 0.03709(H_2/D)^{-0.19}, \quad d/D = 1/3, \quad Re_M > 5.0 \cdot 10^3. \quad (8)$$

The mean frequency of primary circulation characterizes the mean, stable circulation loop. The mean frequency of macroinstability occurrence \bar{f} characterizes, however, an unstable circulation loop, and under turbulent regime of flow it does not depend, in

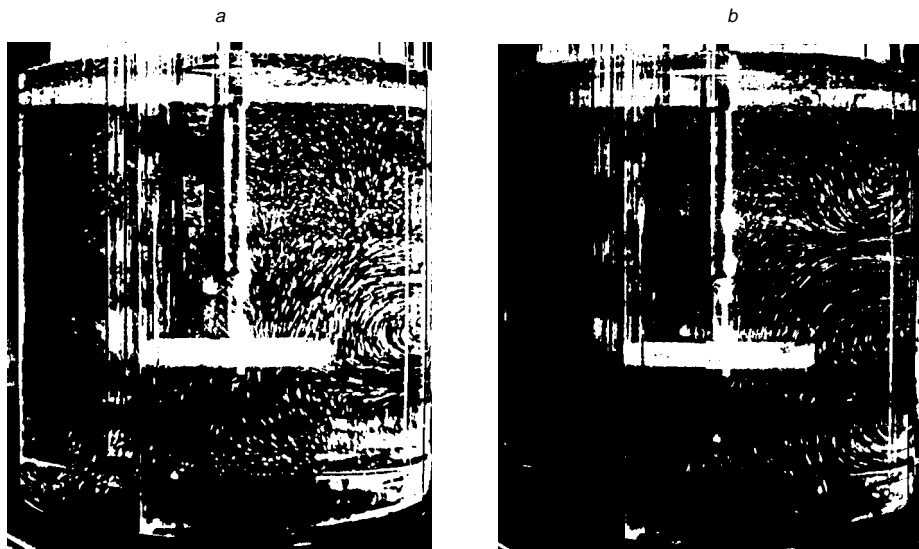


FIG. 7

Photograph of visualized flow field. Agitated liquid – 70% aqueous glycerol solution, temperature 23 °C, frequency of impeller revolution $N = 5.8 \text{ s}^{-1}$, $Re_M = 1\,160$: *a* main flow loop and originating unstable secondary vortex, *b* developed unstable secondary vortex in upper part of vessel

dimensionless form \bar{f}^* , on the Reynolds mixing number (see Fig. 2). Table II consists of both dimensionless frequencies F_c (calculated from Eq. (8)) and f^* (calculated from Table III of the preceding paper²) for all the investigated impeller off-bottom clearances over all the selected liquids and frequencies of impeller revolution:

$$f^* = \sum_{i=1}^{N^*} \frac{f_i}{N_i^*}, \quad H_2/D = \text{const}, \quad Re_M > 5.0 \cdot 10^3. \quad (9)$$

Similarly, number of experimental data N_c of the impeller flow rate number K_p expresses the number of experiments for determination of this quantity¹³ under selected geometric conditions (H_2/D). It follows from results of both experimental studies^{2,13} summarized in Table II that within their accuracy the mean frequency of the primary circulation of agitated liquid is the same as the mean frequency of the macroinstability occurrence. It means that the mean time of the secondary unstable loop occurrence is the same as the mean time of primary stable circulation t_c . From the dependence of the quantity F_c on the simplex H_2/D it is possible to expect higher values of the mean time of the secondary loop occurrence with increasing impeller off-bottom clearance.

CONCLUSIONS

The experiments proved that the macroinstability occurrence in the examined mixing system has its unique laws which can be expressed by the dependence of the dimensionless frequency of their occurrence on the Reynolds mixing number. The form of this dependence is different in the region of developed turbulence than in the transient region. In a pure laminar region, macroinstabilities do not occur. The experiments further made it possible to describe the geometry of flow in the region close under impeller, and their results suggested a possible connection between the formation of macroinstabilities and the instability of flow leaving the impeller. It follows from two sets of the independent experimental results that the mean time of the macroinstability

TABLE II

Dimensionless frequency of primary circulation F_c and dimensionless frequency of the flow macroinstability occurrence f^* under turbulent regime of flow of agitated liquid ($d/D = 1/3$, $H = D$)

H_2/D	K_p^a	F_c	N_c	f^*	N^*
0.20	1.0434 ± 0.104	0.0492 ± 0.0049	16	0.0494 ± 0.0074	15
0.35	0.938 ± 0.094	0.0442 ± 0.0044	16	0.0430 ± 0.0065	15
0.50	0.872 ± 0.087	0.0414 ± 0.0041	16	0.0373 ± 0.0056	15

^a See ref.¹³.

occurrence under the turbulent regime of flow is in a close relation with the mean time of the primary circulation of agitated liquid. The studied phenomenon will apparently influence also the procedure of numerical simulation of turbulent flow of agitated liquid in the system investigated when hitherto the existence of macroinstabilities was not taken into account^{7,14}.

This research was financially supported by the Grant EU Copernicus CIPA-CT-93-0147 "Macroinstabilities in Viscous and Viscoelastic Flows".

SYMBOLS

A	flow field point defined in text
B	flow field point defined in text
b	baffle width, m
D	vessel diameter, m
d	impeller diameter, m
F_c	mean value of dimensionless frequency of primary circulation of agitated liquid
f	mean value of frequency of macroinstability occurrence, s^{-1}
f^*	mean value of dimensionless frequency of macroinstability occurrence
H	liquid height in vessel, m
H_2	impeller off-bottom clearance, m
i	summation index
K_p	impeller flow rate number
N	impeller frequency of revolution, s^{-1}
N_c	number of experimental data of impeller flow rate number
N^*	number of experimental data of frequency of macroinstability occurrence
Re_M	Reynolds mixing number
t	liquid temperature, $^{\circ}C$
t_c	mean time of primary circulation of agitated liquid, s
V	volume of agitated liquid, m^3
\dot{V}	impeller pumping capacity, $m^3 s^{-1}$
β	local flow velocity angle at point B , $^{\circ}$
β_{max}	maximum value of local flow velocity angle at point B , $^{\circ}$
β_{min}	minimum value of local flow velocity angle at point B , $^{\circ}$
δ	local flow velocity angle at point A , $^{\circ}$
μ	liquid viscosity, Pa s
ρ	liquid density, $kg m^{-3}$

REFERENCES

1. Bruha O., Fort I., Smolka P.: Acta Polytech. Czech. Tech. Univ. Prague 33, 27 (1993).
2. Bruha O., Fort I., Smolka P.: Collect. Czech. Chem. Commun. 60, 85 (1995).
3. Winardi S., Nagase Y.: J. Chem. Eng. Jpn. 24, 243 (1991).
4. Kresta S. M., Wood P. E.: Can. J. Chem. Eng. 71, 42 (1993).
5. Ham S., Brodkey R. S.: Ind. Eng. Chem. Res. 31, 1348 (1992).
6. Chapple D., Kresta S.: Chem. Eng. Sci. 49, 3651 (1994).

7. Bakker A., van den Akker H. E. K.: *Trans. Inst. Chem. Eng.*, A 72, 583 (1994).
8. Myers K. J., Ward R. W., Bakker A., Fasano J. B.: Presented at *MIXING XV, The 15th Biennial North American Mixing Conference, Banff (Al, Canada) 1995*.
9. Nouri J. M., Whitelaw J. H.: *AIChE J.* 36, 627 (1990).
10. Green H. L., Carpenter C.: *Proc. 4th Europ. Conf. on Mixing, Noordwijkerhout, Netherlands, April 1982*, pp. 109–126. BHRA Fluid Engineering, Cranfield (U.K.) 1982.
11. Porcelli J. V., Marr G. R.: *Ind. Eng. Chem., Fundam.* 1, 172 (1962).
12. Fort I.: *Collect. Czech. Chem. Commun.* 32, 3663 (1967).
13. Fort I., Sedlakova V.: *Collect. Czech. Chem. Commun.* 33, 836 (1968).
14. Ranade V. V., Mishra V. P., Saxaph V. S., Deshpandi G. B., Joshi J. B.: *Ind. Eng. Chem. Res.* 31, 2370 (1992)